Iranian Journal of Electrical and Electronic Engineering 03 (2020) 302–312
Special Issue on Smart Grids

IUST
Iran University of
Science and Technology

Iranian Journal of Electrical and Electronic Engineering

Journal Homepage: ijeee.iust.ac.ir

Research Paper

Fault Location in Active Distribution Networks Using Improved Whale Optimization Algorithm

A. Bahmanyar*, H. Borhani-Bahabadi*, and S. Jamali*(C.A.)

Abstract: To realize the self-healing concept of smart grids, an accurate and reliable fault locator is a prerequisite. This paper presents a new fault location method for active power distribution networks which is based on measured voltage sag and use of whale optimization algorithm (WOA). The fault induced voltage sag depends on the fault location and resistance. Therefore, the fault location can be found by investigation of voltage sags recorded throughout the distribution network. However, this approach requires a considerable effort to check all possible fault location and resistance values to find the correct solution. In this paper, an improved version of the WOA is proposed to find the fault location as an optimization problem. This optimization technique employs a number of agents (whales) to search for a bunch of fish in the optimal position, i.e. the fault location and its resistance. The method is applicable to different distribution network configurations. The accuracy of the method is verified by simulation tests on a distribution feeder and comparative analysis with two other deterministic methods reported in the literature. The simulation results indicate that the proposed optimized method gives more accurate and reliable results.

Keywords: Fault Location, Optimization, Self-Healing, Smart Grids, Whale Optimization Algorithm.

1 Introduction

MEDIUM-VOLTAGE (MV) distribution networks consist of overhead lines and underground cables, widely spread over rural and urban areas feeding a large number of customers. Such vast networks are vulnerable to faults caused by adverse weather conditions, bird contact, bush fire, etc. After the occurrence of any permanent fault, in order to restore the supply, the maintenance crew has to inspect the lines to find and rectify the fault. Fault location methods can help to accelerate this process and reduce customer outage time. For transient faults, fault location is also required to give an indication of weak points of the network which could eventually lead to permanent faults.

Over the past decades, considerable studies have been devoted to the development of methods to locate short circuit faults in distribution networks [1]. The proposed techniques can be classified into impedance-based methods [2-5], traveling waves-based techniques [6, 7], artificial intelligence-based methods [8, 9], methods using sparse measurements [10-14], and integrated methods [15-17]. Impedance-based methods usually provide multiple estimations for each fault and may cause confusion for operators. Moreover, they are extremely sensitive to network parameter errors. Travelling waves-based techniques require measurements with very high sampling frequencies which are expensive at the distribution level. The main shortcoming of all learning-based approaches is the requirement of retraining for any changes in the distribution network topology. Integrated methods need the requirements of all of the methods which are integrated [1].

Locating the short circuit faults is not an optimization problem in concept, however, optimization algorithms can be used as a tool to solve it. Therefore, over the last

Iranian Journal of Electrical and Electronic Engineering, 2020.
Paper first received 29 October 2019, revised 06 February 2020, and accepted 11 February 2020.
* The authors are with the Center of Excellence for Power System Automation and Operation, Iran University of Science and Technology (IUST), School of Electrical Engineering, Tehran, Iran.
E-mails: bahmanyar@iust.ac.ir, h_borhani@elec.iust.ac.ir, and sjamali@iust.ac.ir.
Corresponding Author: S. Jamali.

years, a new class of fault location methods is proposed which benefits from the optimization techniques to solve the fault location problem [18-24]. The authors of [18], first identify the faulty feeder using the zero-sequence voltages at both terminals of each feeder. A golden section search algorithm is then adopted to identify the faulted section and the genetic algorithm is used to locate the fault. In [19] an immune algorithm-based optimization method is proposed for faulted section estimation using the information of the status of protective relays and circuit breakers. In [20] the authors present a faulted line detection method for non-effectively grounded networks, based on an optimized bistable system. These methods present acceptable results; however, they do not consider the presence of Distributed Energy Resources (DER).

In smart grids, the presence of DER changes the direction of power flows and complicates the protection and control. The optimization-based method proposed in [21] considers the presence of DER in distribution networks. The method finds the fault location as an optimal solution using the genetic algorithm. In [22], the authors propose a method which combines genetic algorithm with binary particle swarm optimization to locate single-phase to ground faults in overhead distribution feeders with DER. The method uses the mutation direction differences of the transient zero sequence current and voltage of each line-section to find the faulted one and then solves a fault distance equation to locate it. These methods only locate single-phase to ground faults.

The method proposed in [23] is mainly impedance-based and relies on the minimum fault reactance concept. It solves a fault location equation for all network line-sections as a minimization problem and uses a Fibonacci-based search technique to improve the estimation process. The authors of [24] present a fault location method for distribution networks with DER units, which relies on an optimization process that estimates the fault location using the pattern search method. The proposed method is based on voltage and current phasor quantities, calculated from measurements taken only at the substation. In its optimization process, the method estimates the fault distance and impedance quantities that minimize the error between the estimated post-fault voltages phasor quantities and the measured ones. While the proposed method provides acceptable results, it faces the multiple solution problem, and in 25% of studied cases, the correct solution is not between the first four ranked line sections.

Among the previously optimization-based fault location methods, the methods of [18-20] do not consider the presence of DER, the methods proposed in [21, 22] are only applicable for single-phase to ground faults, and the method of [23,24] may face the multiple solution problem. In this paper, a combination of an optimization algorithm and recorded voltage sag is proposed to achieve a better performance compared with the aforementioned techniques. After several trials of different optimization techniques, an improved WOA is presented to find the optimal solution.

The rest of the paper is organized as follows: In Section 2, the optimization problem and the fitness function are defined. Section 3 presents the details of the improved WOA. Simulation studies are given in Section 4 where the performance of the proposed method is evaluated and Section 5 concludes the paper.

2 Fault Location as an Optimization Problem

Following to any short circuit fault in the network, voltages of all network nodes decrease. The fault location methods proposed in [10-13] are based on the fact that faults occurring at different locations, will result in different voltage sag magnitudes at each network node. Therefore, having the measured voltage sags at some of the nodes, it would be possible to find the fault location. The methods first consider the fault at each node, run a distribution load flow, and calculate the voltage sags at the nodes with measurement devices. Then, they identify the node with the maximum similarity between the calculated and measured voltage sags as the fault location. The similarity can be evaluated by the following equations:

$$\sigma_i = \sum_{j=1}^{m} \sum_{a,b,c} \left| \Delta V_{i,j}^{calc} - \Delta V_{j}^{meas} \right| \tag{1}$$

$$\Delta V = \left| V^{f} \right| - \left| V^{pre} \right| \tag{2}$$

where V^{pre} and V^{f} represent the pre-fault and fault voltages, ΔV_j^{meas} is the voltage sag magnitude measured at node j, $\Delta V_{i,j}^{calc}$ is the voltage sag magnitude at node j when fault is considered at node i, which can be calculated by a distribution load flow.

For each node, σ is the sum of the difference between the calculated and measured voltage sags for three-phase and m measurement nodes as represented in (1). The node with the minimum value of σ is the fault location.

For any short circuit fault, there are two unknown variables. The first one, which is of great interest to electricity distribution companies, is fault location. The second one is fault impedance, which has a resistive nature. Therefore, during a short circuit fault, measured voltages and currents at any point x of the network can be written as a function of fault location (L_f) and fault resistance (R_f):

$$V_x = f\left(L_f, R_f\right) \tag{3}$$

$$I_x = g\left(L_f, R_f\right) \tag{4}$$

As shown in Fig. 1, R_f represents a set of fault resistance values which can vary from zero to infinity, depending on the fault type and the phases involved. For example, for a phase ‘a’ to ground fault, r_f takes a nonzero unknown value and the values of r_a, r_b and r_c are zero, infinity and infinity, respectively.

Consider the distribution network shown in Fig. 2. For a single-phase to ground fault at node 72 with r_f = 20Ω, based on (2), fault location and fault resistance are the variables which determine the magnitude of the fault induced voltage sags at different network nodes. By applying the fault at all network nodes with different fault resistance values, the σ values calculated using (1), form a surface in (L_f, r_f, σ) space (Fig. 3). For better presentation of this 3-dimensional space for different fault location and resistance values, Fig. 4 presents its projection in 2-dimensional planes. As can be seen, the minimum σ value is associated with node 72 and 20Ω fault resistance which are the correct fault resistance and location.

Therefore, by considering the fault at all network nodes with different fault resistance values, and calculating the σ values, fault location and resistance values for which the calculated σ is the minimum, can be considered as the correct solution. However, investigation of all possible fault location and resistance values imposes a high computational burden, thus, more optimized methods are preferred. After several trials of different optimization techniques, the whale optimization algorithm is chosen as an efficient technique to solve the aforementioned problem. For any short circuit fault in electricity distribution networks, there is a surface as shown in Fig. 3, for which the presented optimization algorithm searches the global minimum.

3 Improved Whale Optimization Algorithm

The whale optimization algorithm is a new meta-heuristic algorithm proposed in [25]. The algorithm is based on the humpback whales behavior and strategy for catching fish using a bubble network. In the strategy of the bubble network, a whale creates a '9'-shaped path of bubbles around a bunch of fish. With a spiral upward motion, the whale begins to produce bubbles about 12 meters below the fish and gradually moves towards the surface in a spiral path. Fig. 5 shows an illustration of humpback whales strategy for fish hunting.

The hunter can detect the overall position of the fish and loop around it. Since the optimal location is initially unknown, the WOA assumes that the current position is the best position. After determining the whale with the best position, other whales update their position based on it. This behavior is shown in the form of the following relationships:

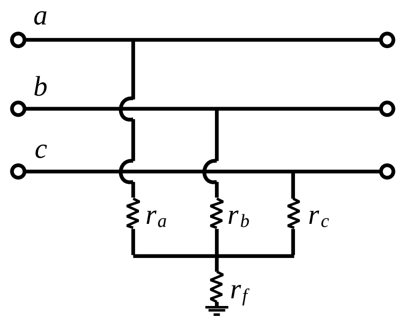

Fig. 1 Short circuit fault model.

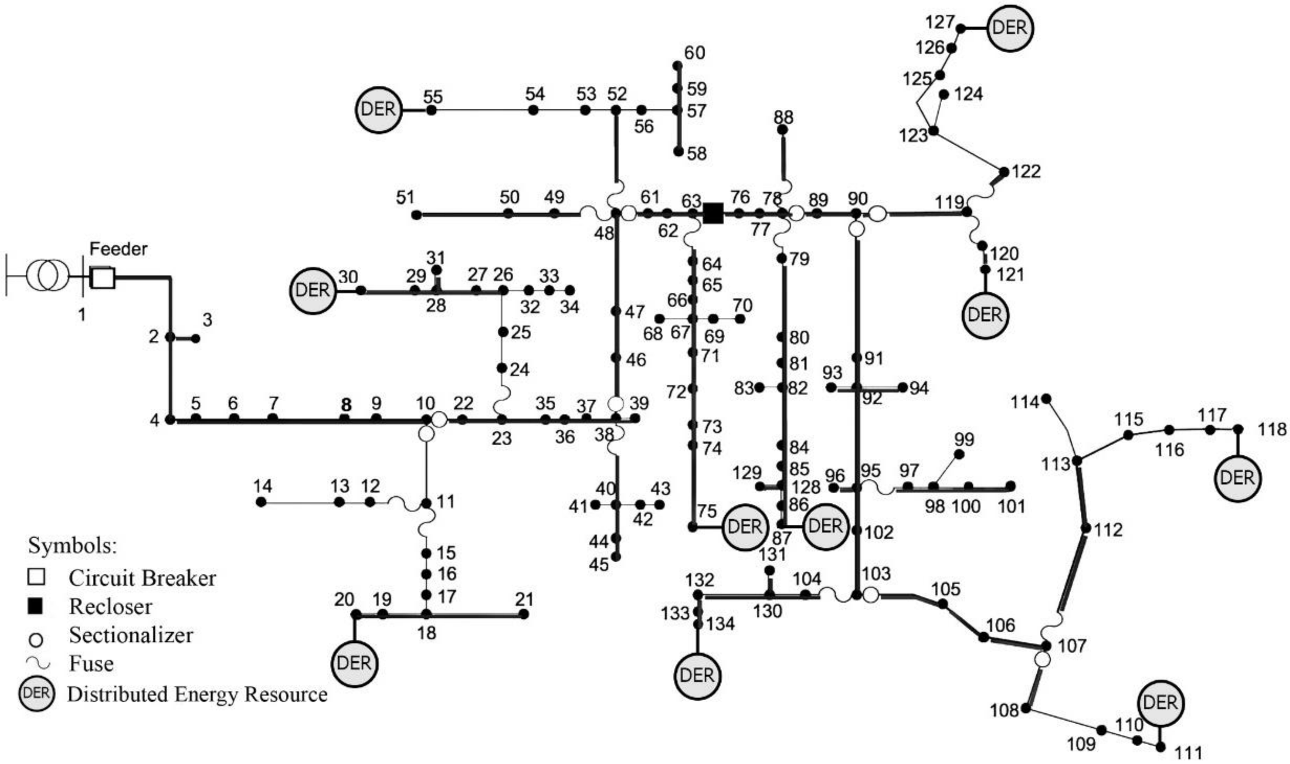

Fig. 2 Practical 134-node distribution feeder with several DER units [13].

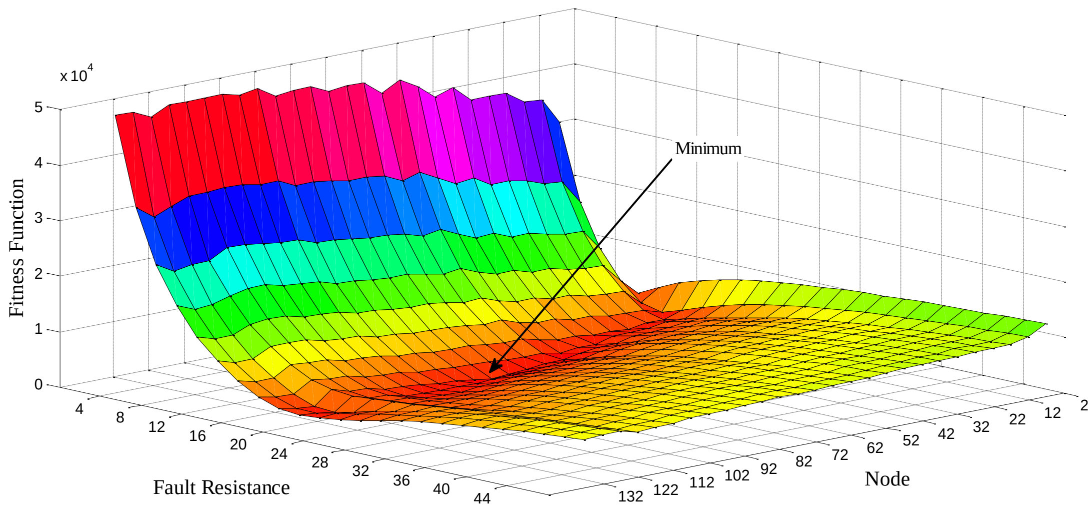

Fig. 3 Calculated σ values in (L_f, r_f, σ) space.

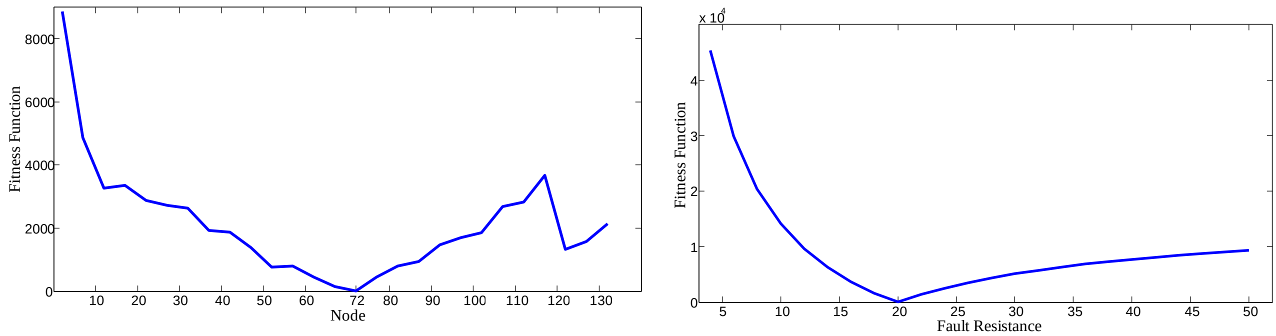

(a) (b)

Fig. 4 Calculated σ values: a) in (L_f, σ) plane for $r_f = 20\Omega$ and b) in (r_f, σ) plane for fault at node 72.

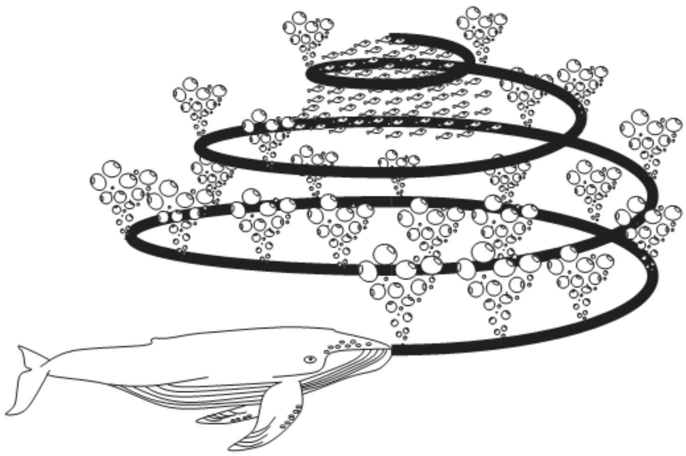

Fig. 5 Humpback whales bubble network strategy for fish hunting [25].

$$\vec{D} = \left|\vec{C} \cdot \vec{X}^*(t) - \vec{X}(t)\right| \tag{5}$$

$$\vec{X}(t+1) = \vec{X}^*(t) - \vec{A} \cdot \vec{D} \tag{6}$$

where t represents the current iteration, D is the distance between the current position and the best position, A and C are the vector of coefficients, X is the position vector and $X*$ is the position vector of the best solution. '| |' represents the absolute value and '.' is the inner product. It is necessary to emphasize that $X*$ is updated at each iteration.

The vectors A and C are calculated as follows:

$$\vec{A} = 2\vec{a} \cdot \vec{r} - \vec{a} \tag{7}$$

$$\vec{C} = 2 \cdot \vec{r} \tag{8}$$

where a decreases linearly from 2 to 0 during the iterations and r is a random vector in the range between 0 and 1.

3.1 Attack Method With Bubble Network

The behavior of the humpback whale bubble network is formulated in two steps:

Step 1: Helix ring mechanism

This behavior is obtained by reducing the value of a in (7). Therefore, with respect to (7), the value of A also decreases.

Step 2: Updated spiral path position

For updating the spiral path position, first the distance between the whale at position (X, Y) and target hunting (X^*, Y^*) is calculated. The equation to model the spiral movement of the whale is as follows:

$$\vec{X}(t+1) = \vec{D}' \cdot e^{bl} \cdot \cos(2\pi l) + \vec{X}^*(t) \tag{9}$$

where $\vec{D}'$ represents the distance between each whale to the target (the best solution so far). The b constant is used to determine the spiral logarithmic slope, and l is a random number between 0 and 1.

In order to create more dynamics in the algorithm, in this paper, instead of using a fixed value, the following equation is proposed to determine the value of b:

$$b = t \times r^t \tag{10}$$

where t is the current iteration and r is a random number between 0 and 1.

Humpback whale swims around its hunt in a spiral path. The following equation represents this behavior:

$$\vec{X}(t+1) = \begin{cases} \vec{X}^*(t) - \vec{A} \cdot \vec{D} & \text{if } p < 0.5 \\ \vec{D}' \cdot e^{bl} \cdot \cos(2\pi l) + \vec{X}^*(t) & \text{if } p \geq 0.5 \end{cases} \tag{11}$$

where p is a random value between 0 and 1.

In order to show the effect of the proposed improvement in (10) on the algorithm convergence, Fig. 6 represents the objective value at different iterations. As can be seen in the figure, by selecting the b value based on (10), instead of using a fixed value, the X quickly converges.

3.2 Search for Fish

A method based on the change of vector A can be used to search for fish. In fact, the humpback whales are doing the search randomly in separate areas. In order to model this, random values of more than 1 or less than -1 are chosen for A, to make whales to search for the best solution in different areas.

The mathematical model of this behavior is as follows:

$$\vec{D} = \left| \vec{C} \cdot \vec{X}_{rand} - \vec{X} \right| \tag{12}$$

$$\vec{X}(t+1) = \vec{X}_{rand} - \vec{A} \cdot \vec{D} \tag{13}$$

where X_{rand} is a random position vector (random whales).

3.3 Stopping Criteria

The process is being repeated until the variations of $\sigma(X^*)$ is less than a predefined threshold (ε).

Fig. 7 shows the flowchart of the proposed optimization-based fault location method. With the occurrence of any fault in the distribution network, the

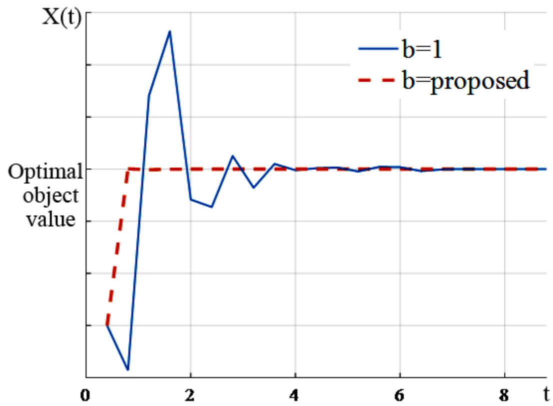

Fig. 6 Objective value at different iterations.

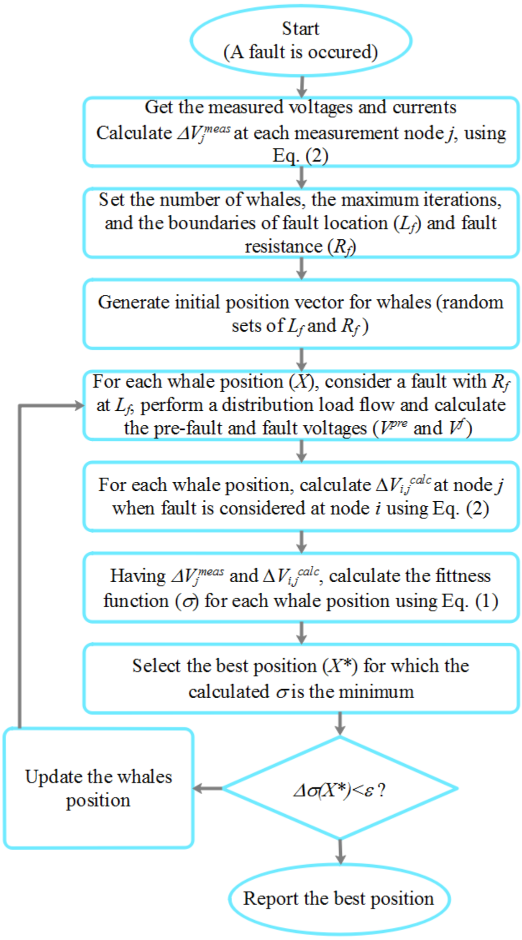

Fig. 7 Flowchart of the proposed algorithm.

proposed fault location method initially selects a random value for fault resistance and faulted node. Then, using the optimization algorithm described, the minimum fitness function is searched to determine the correct values of the fault location and resistance.

4 Results and Discussion

To evaluate the performance of the proposed method, several tests are performed on the simulated model of the 134-node distribution feeder of Fig. 2 [13]. The test system is simulated in ATP_EMTP software. To consider the distributed energy resources, 10 DER units are connected at different nodes. These present the distributed generation units or microgrids that remain connected for some cycles during the fault. It is assumed that the voltage and currents measured at the head of the main feeder and all the DER terminals are available through a reliable communication infrastructure. The full cycle discrete Fourier transform is employed to calculate the fundamental phasors of measurement waveforms. The method is tested for different fault locations, fault types and fault resistances and the obtained results are compared against the voltage sag-based methods proposed in [10, 11].

Consider a single-phase to ground fault at Node 40 with $r_f = 10\Omega$. The fault location method proposed in [11] first estimates the fault current as the sum of the contributions of all sources and then considers the fault at all network nodes and calculates the following λ index for each of them. The node with the minimum value of λ has the minimum difference between the calculated and measured voltage sags and would be the fault location.

$$\lambda_i = \sum_{j=1}^{m} norm\left(\Delta V_{i.j}^{calc} - \Delta V_j^{meas}\right) \tag{14}$$

where m is the number of measurements, ΔV is as defined in (2) and the norm is calculated as follows:

$$\text{norm}(X) = \left[\left|X(1)\right|^2 + \left|X(2)\right|^2 + \ldots + \left|X(k)\right|^2\right]^{1/2} \tag{15}$$

The calculated λ values under the considered fault scenario are presented in Fig. 8. The minimum value is associated with node 46 which is 160m away from the fault location. The estimation error is due to the methods approximate estimation of fault current.

The fault location method proposed in [10] calculates the fault current as the difference between the source currents and load currents during load flow iterations. The method considers the fault at all network nodes and calculates the following η index for each node. The node with the maximum value of η is the one with the minimum difference between the calculated and measured voltage sags and would be the fault location.

$$\eta_j = \frac{1}{\max\left(\max\left(\delta_{i,j}\right) - \min\left(\delta_{i,j}\right)\right) + \Delta} \tag{16}$$

where $\delta_{i,j}$ is defined as follows and ΔV is as defined in (2).

$$\delta_{i,j} = \Delta V_j^{meas} - \Delta V_{i,j}^{calc} \tag{17}$$

The calculated η values are presented in Fig. 9. The maximum value is associated with node 43 which is 60 m away from the fault location. For this fault scenario, the estimation error of the method proposed in [10] is less than the method proposed in [11].

Unlike the previous methods, the proposed method does not need to consider all the network nodes. It estimates the fault location and resistance values through the minimization of the fitness function of (1) via an optimization process.

For WOA settings, the number of search agents (whales) is set to 30, the maximum number of iteration is set to 50. The variables (whale position) are the set of fault resistances and faulted node. The considered search interval of fault resistance is from 0 to 150 ohms. Also, the search interval for the faulted node is from 1 to the number of network nodes.

For the single-phase to ground fault at node 40 with $r_f = 10\Omega$, as shown in Fig. 10, the WOA requires 29 iterations to find the minimum of the fitness function which is associated with the correct answer. While, the improved WOA proposed, only requires 7 iterations to find the correct solution.

4.1 Effect of Fault Distance, Resistance and Type

To study the effect of the fault resistance on the proposed method, single-phase to ground faults with different fault resistance values are simulated at different locations and the obtained results are presented

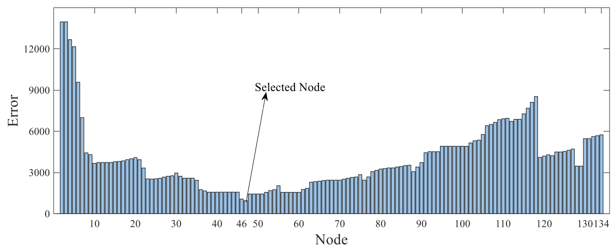

Fig. 8 Calculated λ values for the method proposed in [11].

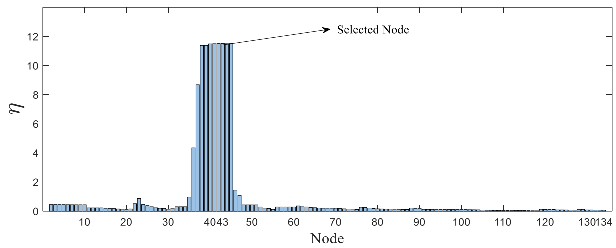

Fig. 9 Calculated η values for the method proposed in [10].

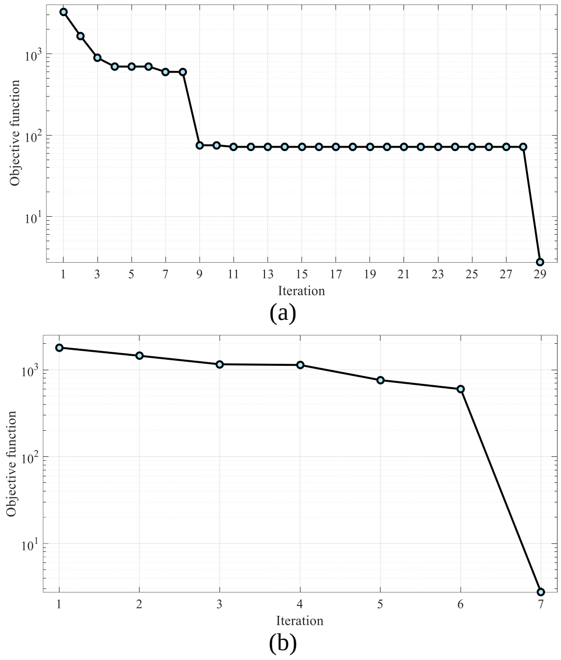

Fig. 10 Fitness function in each optimization iteration: a) WOA and b) improved WOA.

in Table 1, which presents the faulted node identified by each method. In most of the fault scenarios, the method proposed in [11] is not able to identify the faulted node. The method proposed in [10] presents comparatively more accurate results, but, in some cases it cannot differentiate between neighboring nodes to find the faulted one.

The results indicate the use of the proposed optimization-based method provides more accurate results. In all of the considered scenarios, the selected node is either the faulted node or its adjacent node.

Fig. 11 presents the distance between the faulted node and the node identified by the fault location method in meter (*error*) for different fault resistance values. The results indicate that the change of fault resistance does not have a considerable effect on the accuracy of the method. Fig. 12, represents the error for different values of fault distance from the main substation. Based on the results, for all the considered fault distance and resistance values, using the optimization technique improves the fault location accuracy. The mean errors for the method of [11], the method of [10] and the proposed method are 223, 67, and 10.25 meters respectively.

For single-phase to ground faults, depending on the phases involved, r_a, r_b and r_c in Fig. 1 are zero or infinity and r_f is a nonzero unknown value. Therefore, for this type of short circuit faults, r_f and fault location (L_f) are the only unknown values that should be estimated during the optimization process. However, for three-phase to ground faults, r_a, r_b, r_c, r_f, and L_f are all unknowns to be estimated. Therefore, for this type of fault, the optimization surface is in a 6-dimentional space instead of the 3-dimentional space of Fig. 3.

Table 2 presents the fault location results for three-phase to ground faults with different fault resistance values. Also for this type of fault, the proposed method presents more accurate results in all fault scenarios.

Table 1 Results of the fault location methods for single-phase to ground faults.

Method	R_f [Ω]	Fault node							
		7	12	40	56	72	101	112	129
Method of [10]		7	14	43	52	72	95	112	128
Method of [11]	5	6	22	46	75	88	103	113	89
Proposed Method		7	12	40	56	72	101	112	129
Method of [10]		7	14	43	60	72	101	112	129
Method of [11]	10	6	22	46	75	88	103	113	89
Proposed Method		7	12	40	56	72	101	112	128
Method of [10]		7	12	43	60	72	101	112	129
Method of [11]	20	6	22	46	75	88	103	113	89
Proposed Method		7	12	41	56	72	101	112	129
Method of [10]		7	14	43	60	72	95	112	128
Method of [11]	50	6	22	46	75	77	103	113	89
Proposed Method		7	13	44	56	72	101	112	128
Method of [10]		7	14	43	60	72	95	112	128
Method of [11]	100	6	22	46	75	77	103	113	89
Proposed Method		7	13	41	52	72	101	112	128

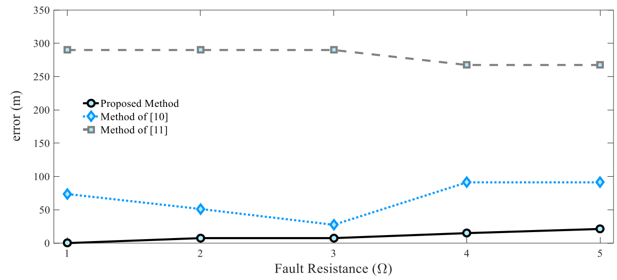

Fig. 11 Estimation error of different fault location methods for different fault resistance values in meter.

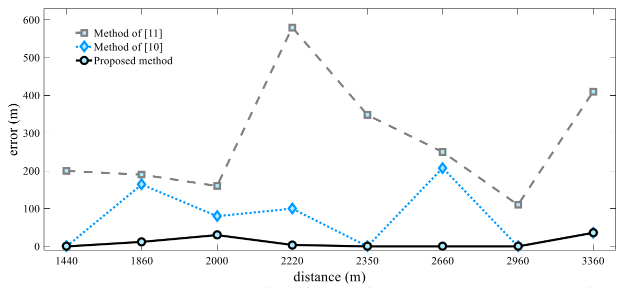

Fig. 12 Estimation error of different fault location methods for different fault distance values in meter.

Table 2 Results of the fault location methods for three-phase to ground faults.

Method	R_f [Ω]	Fault node							
		7	12	40	56	72	101	112	129
Method of [10]	r_f=10 ra=3 r_b=4 r_c=5	7	14	44	57	72	96	111	85
Method of [11]		6	14	46	62	77	102	113	89
Proposed Method		7	12	44	57	72	101	113	85
Method of [10]	r_f=25 r_a=5 r_b=3 r_c=6	7	10	45	57	71	96	112	85
Method of [11]		6	14	46	62	77	102	112	86
Proposed Method		7	12	44	57	73	101	112	128

4.2 Effect of Load Data Uncertainty

Distribution network loads change by time considerably and hence the available load data of electricity distribution networks are uncertain and inaccurate. Therefore, to test the practicality of fault location methods, their performance with erroneous load data should be studied. To test the effect of load data inaccuracies on the fault location results, load data employed for the simulations is taken as a benchmark and the erroneous load data is generated by random variation of them:

$$S_j = S_j^a \left(1 + \varepsilon_j e_L\right) \tag{18}$$

where S_j^a and ε_j are load apparent power of node j and a random number between -1 to 1 respectively, and e_L is the range of deviation considered.

Table 3 presents the fault location results for single-phase to ground faults with 30% error in load data (e_L = 0.3). A comparison of the results of this table with the results under ideal conditions in Table 1 shows that for low fault resistance values, load data errors do not affect the accuracy of the proposed method. But for high fault resistance values, the estimation accuracy is decreased. However, the proposed optimization-based method can maintain its accuracy in an acceptable range and in most of the considered fault scenarios, its results are more accurate than the other methods.

4.3 Effect of Meters Quantity and Location

In all of the previous case studies, it was assumed that meters are placed at the head of the main feeder and all the DER terminals (i.e. nodes 20, 30, 55, 75, 87, 111, 118, 121, 127, and 134). In this section, two other cases are considered to evaluate the performance of the proposed method for different meter locations and with fewer meters.

Case (1) Five metering points at the terminals of DERs at nodes 20, 55, 87, 118, and 127.

Case (2) Ten metering points at the terminals of DERs at nodes 14, 34, 58, 70, 83, 90, 108, 114, 124, and 131.

Case (1) is designed to study the effect of the number of measurements, while Case (2) is designed to evaluate the performance of the proposed method for different meter locations. As shown in Table 4, compared to the base case, the method provides less accurate results with fewer measuring points. However, in all the considered fault scenarios the results are satisfactory. In the worst case, for a fault at node 7, the proposed method selects node 22 which is just 4 nodes and 290 meters away. With the same number of measuring points, but at different locations in Case (2), almost the same results as the base case are obtained. The mean errors for the base case, Case (1) and Case (2) are 15, 76, and 20 meters respectively. Therefore, the location of the meters may influence the method performance. However, the method can provide satisfactory results even with a few numbers of meters, as long as the meters are well distributed over the network.

Table 3 Results of the fault location methods with 30% error in load data.

Method	R_f [Ω]	Fault node							
		7	12	40	56	72	101	112	129
Method of [10]	5	7	14	38	52	72	95	112	128
Method of [11]		7	23	47	76	89	104	114	90
Proposed Method		7	12	40	56	72	101	112	129
Method of [10]	20	7	14	47	52	72	95	112	128
Method of [11]		7	23	38	76	89	104	114	90
Proposed Method		7	12	40	52	72	101	112	86
Method of [10]	100	6	14	38	60	72	95	112	128
Method of [11]		6	23	47	76	78	104	113	90
Proposed Method		7	13	39	52	72	100	112	85

Table 4 Results for different numbers and locations of meters (single-phase to ground faults with R_f=50Ω).

Case	Fault node							
	7	12	40	56	72	101	112	129
Base case	7	13	44	56	72	101	112	128
Case 1	22	13	39	56	71	101	112	85
Case 2	7	12	44	56	72	101	112	87

4.4 Comparison With Other Optimization Algorithms

In this section, a comparison is made between the proposed method and other optimization algorithms in terms of fault location accuracy and convergence speed, for faults at 8 locations and with 5 different fault resistances (fault scenarios of Table 1). For this comparison, each algorithm is run 20 times for each fault scenario (800 runs in total for each algorithm). Table 5 compares different algorithms in terms of

Table 5 Results of comparison with different optimization algorithms.

	Genetic algorithm	Partial swarm optimization	WOA	Improved WOA
Estimation error [m]				
Maximum	110	110	60	60
Average	35	32.5	18.75	10.25
Minimum	0	0	0	0
Iterations				
Maximum	41	48	36	18
Average	32	29	22	8
Minimum	12	15	9	1

estimation error and convergence speed. In general, the improved WOA algorithm is more accurate and requires less number of iterations to locate the fault.

5 Conclusions

This paper presents a new fault location method for active power distribution networks which is based on measured voltage sag and use of an improved WOA. The proposed method is applicable to distribution networks with several laterals and load taps and it provides a single solution. Simulation tests verify the accuracy of the proposed method for different fault types, fault resistances and fault positions. Comparative studies are presented with two other deterministic voltage sag-based methods for different fault conditions to investigate the benefits of using optimization. The results indicate that the use of the presented optimization algorithm has considerably decreased the estimation error, say, from the average 223 and 67 meters in case of deterministic methods to around 10 meters. The results also indicate that the method is able to maintain its accuracy under load data errors, and with a few numbers of meters at different locations.

In brief, the main contribution can be summarized as follows:

1. The method is conceptually simple and can be implemented in large branched distribution networks with several load taps and laterals;
2. In contrast to the previous optimization-based methods [18-24], the proposed method can be applied to distribution networks with DER without requiring their information, it does not face the multiple solution problem and it gives accurate results for different fault types;
3. In comparison with the deterministic voltage sag-based techniques [10-13], which need to calculate the fault impedance or its current for fault location, the proposed method does not require such calculations and provides comparatively more accurate results;
4. Even when accurate data of distribution network loads are not available, which is a common practical implementation barrier, the proposed method can maintain its accuracy in an acceptable range.
5. Simulation studies show that the proposed method can provide satisfactory results even with a fewer number of meters, as long as the meters are well distributed over the network. Moreover, comparisons with other optimization algorithms show the superiority of the proposed method in terms of accuracy and convergence.

In general, the proposed method provides accurate results for active distribution network faults with different types, locations, and resistances, even with erroneous load data, showing its potential to help to realize the self-healing concept.

References

[1] A. Bahmanyar, S. Jamali, A. Estebsari, and E. Bompard, "A comparison framework for distribution system outage and fault location methods," *Electric Power Systems Research*, Vol. 145, pp. 19–34, 2017.

[2] E. Correa-Tapasco, J. Mora-Flórez, and S. Pérez-Londoño, "Robustness of a generalized impedance based fault locator considering distorted measurements," *Electric Power Systems Research*, Vol. 154, pp. 234–244, 2018.

[3] C. Orozco-Henao, A. Bretas, A. Herrera-Orozco, J. Pulgarín-Rivera, S. Dhulipala, and S. Wang, "Towards active distribution networks fault location: contributions considering DER analytical models and local measurements," *International Journal of Electrical Power & Energy Systems*, Vol. 99, pp. 454–464, 2018.

[4] A. Bahmanyar and S. Jamali, "Fault location in active distribution networks using non-synchronized measurements," *International Journal of Electrical Power & Energy Systems*, Vol. 91, pp. 451–458, 2017.

[5] R. Dashti, M. Ghasemi, and M. Daisy, "Fault location in power distribution network with presence of distributed generation resources using impedance based method and applying π line model," *Energy*, Vol. 159, pp. 344–360, 2018.

[6] D. Jalali and N. Moslemi, "Fault location for radial distribution systems using fault generated high-frequency transients and wavelet analysis," in *18th International Conference and Exhibition on Electricity Distribution (CIRED)*, pp. 1–4, 2005.

[7] X. Wang, G. Song, Z. Chang, J Lou, J Gao, X Wei, and Y. Wei, "Faulty feeder detection based on mixed atom dictionary and energy spectrum energy for distribution network," *IET Generation, Transmission & Distribution*, Vol. 12, No. 3, pp. 596–606, 2017.

[8] D. Thukaram, H. Khincha, and H. Vijaynarasimha, "Artificial neural network and support vector machine approach for locating faults in radial distribution systems," *IEEE Transactions on Power Delivery*, Vol. 20, No. 2, pp. 710–721, 2005.

[9] A. Rafinia and J. Moshtagh, "A new approach to fault location in three-phase underground distribution system using combination of wavelet analysis with ANN and FLS," *International Journal of Electrical Power & Energy Systems*, Vol. 55, pp. 261–274, 2014.

[10] R. Pereira, L. Silva, M. Kezunovic, and J. Mantovani, "Improved fault location on distribution feeders based on matching during-fault voltage sags," *IEEE Transactions on Power Delivery*, Vol. 24, No. 2, pp. 852–862, 2009.

[11] S. Brahma, "Fault location in power distribution system with penetration of distributed generation," *IEEE Transactions on Power Delivery*, Vol. 26, No. 3, pp. 1545–1553, 2011.

[12] S. Lotfifard, M. Kezunovic, and M. J. Mousavi, "Voltage sag data utilization for distribution fault location," *IEEE Transactions on Power Delivery*, Vol. 26, No. 2, pp. 1239–1246, 2011.

[13] F. Trindade, W. Freitas, and J. Vieira, "Fault location in distribution systems based on smart feeder meters," *IEEE Transactions on Power Delivery*, Vol. 29, No. 1, pp. 251–260, 2014.

[14] S. Jamali, A. Bahmanyar, and E. Bompard, "Fault location method for distribution networks using smart meters," *Measurement*, Vol. 102, pp. 150–157, 2017.

[15] S. Alwash, V. Ramachandaramurthy, and N. Mithulananthan, "Fault location scheme for power distribution system with distributed generation," *IEEE Transactions on Power Delivery*, Vol. 30, No. 3, pp. 1187–1195, 2015.

[16] E. Reche, J. De Sousa, D. Coury, and R. Fernandes, "Data mining-based method to reduce multiple estimation for fault location in radial distribution systems," *IEEE Transactions on Smart Grid*, Vol. 10, No. 4, pp. 3612–3619, 2018.

[17] F. Trindade and W. Freitas, "Low voltage zones to support fault location in distribution systems with smart meters," *IEEE Transactions on Smart Grid*, Vol. 8, No. 6, pp. 2765–2774, 2016.

[18] L. Rui, P. Nan, Y. Zhi, and F. Zare, "A novel single-phase-to-earth fault location method for distribution network based on zero-sequence components distribution characteristics," *International Journal of Electrical Power & Energy Systems*, Vol. 102, pp. 11–22, 2018.

[19] S. J. Huang, "Application of immune-based optimization method for fault-section estimation in a distribution system," *IEEE Transactions on Power Delivery*, Vol. 17, pp. 779–784, 2002.

[20] X. Wang, J. Gao, M. Chen, X. Wei, Y. Wei, and Z. Zeng, "Faulty line detection method based on optimized bistable system for distribution network," *IEEE Transactions on Industrial Informatics*, Vol. 14, No. 4, pp. 1370–1381, 2018.

[21] S. Jamali, A. Bahmanyar, and H. Borhani-Bahabadi, "A Fast and accurate fault location method for distribution networks with DG using genetic algorithms," in *Smart Grid Conference (SGC)*, pp. 110–114, 2015.

[22] T. Jin and H. Li, "Fault location method for distribution lines with distributed generators based on a novel hybrid BPSOGA," *IET Generation, Transmission & Distribution*, Vol. 10, No. 10, pp. 2454–2463, 2016.

[23] C. Orozco-Henao, A. Bretas, R. Chouhy-Leborgne, A. Herrera-Orozco, and J. Marín-Quintero, "Active distribution network fault location methodology: A minimum fault reactance and Fibonacci search approach," *International Journal of Electrical Power & Energy Systems*, Vol. 84, pp. 232–241, 2017.

[24] G. Manassero, S. Di Santo, and L. Souto, "Heuristic method for fault location in distribution feeders with the presence of distributed generation," *IEEE Transactions on Smart Grid*, Vol. 8, pp. 2849–2858, 2017.

[25] S. Mirjalili and A. Lewis, "The whale optimization algorithm," *Advances in Engineering Software*, Vol. 95, pp. 51–67, 2016.

A. Bahmanyar was born in Bojnord, Iran in 1986. He received the M.Sc. degree from Guilan University, Rasht, Iran in 2011, and the Ph.D. degree from Iran University of Science and Technology (IUST), Tehran, Iran in 2017, all in Electrical Engineering. Dr. Bahmanyar is currently with Niroo Research Institute (NRI), the main research organization affiliated to Iran Ministry of Energy. His research interests include modern distribution networks operation, man-made attack modeling, and power system resiliency.

H. Borhani-Bahabadi was born in Bahabad, Yazd, Iran in 1985. He received the B.Sc. and M.Sc. degrees from Yazd University, Yazd, Iran, in 2008 and 2010, respectively, and the Ph.D. degree from the Department of Electrical Engineering at Iran University of Science and Technology (IUST), Tehran, Iran, in 2013. His research interests include protection, operation and planning of distribution systems, integration of distributed generation, and power quality.

S. Jamali received the B.Sc. degree from Sharif University of Technology, Tehran, Iran in 1979, the M.Sc. degree from University of Manchester, UK, in 1986, and the Ph.D. degree from City University, London, UK, in 1990, all in Electrical Engineering. Dr. Jamali is currently with the School of Electrical Engineering at Iran University of Science and Technology (IUST), Tehran, Iran. He is a Fellow of the Institution of Engineering and Technology, UK, and a Chartered Engineer (CEng) in the UK. His research findings have been published in over 200 papers in learned society journals and recognized international conferences. His areas of research interests are power system protection, distribution systems, and railway electrification.